

The quantum optical description of a double Mach-Zehnder interferometer

Stefan Ataman

*ECE Paris, 37 quai de Grenelle, 75015 Paris, France**

In this paper we describe within the formalism of Quantum Optics (QO) a double Mach-Zehnder interferometer (MZI). For single photon Fock states this experimental setup is shown to exhibit a counter-intuitive behavior: for certain values of the path length difference of the first MZI, the singles photon-count statistics at the output detectors does not change, whatever the difference in path length for the second MZI. For simultaneously impinging light quanta, we show that this setup is able to show the same HOM antibunching effect previously obtained with a beam splitter. However, by adding substantial delays in each MZI, we can obtain the same effect even if the “photon wave packets” do not overlap at the second beam splitter.

I. INTRODUCTION

The beam splitter (BS) is one of the most widely used devices in Quantum Optics. This notoriety is partially due to the fact that a beam splitter can transform a non-entangled state into an entangled one [1–4] (and vice-versa), differentiate between a coherent and a Fock state [5, 6] and reveal non-classical features of light [7–9]. Applying a coherent state [10–12] at one input and a single-quantum Fock state at the other one of a BS allows measuring quantum states of light using the homodyne detector [13–15].

In the classical description of a lossless beam splitter, energy conservation imposes the relation between input and output electric fields [1, 3]. In the quantum optical description, fields are replaced by operators [16]. A more general framework has been developed, where beam-splitters are described in SU(2) symmetries [17, 18]. However, authors prefer a subset of this general model, having symmetrical [1, 4] (typically for single layer dielectric beam splitters) or non-symmetrical operator input-output operator relations [2, 3] (typically for cube beam-splitters).

A Mach-Zehnder interferometer (MZI) is a device composed of two beam splitters and two mirrors [1]. Its versatility has led to its use in countless experiments [5, 19, 20, 26]. Applying a single light quantum at one input, the rate of photo-detection oscillates as the path-length difference of the interferometer is swept [5]. However, no coincidence counts are detected. Applying pairs of light quanta at its inputs, specific non-classical effects show up [19].

The special interest in Quantum Optics stems from the fact that it allowed a whole new set of *Gedankenexperiments* to be brought to reality (*e.g.* quantum eraser [21–24] interaction-free measurements [25, 26], quantum-non-demolition (QND) experiments [27]). A review of fundamental experiments in the field of QO is given in Steinberg *et al.* [28].

The so-called “semi-classical” approach [2, 3] in QO ex-

plains many aspects of light (including the photo-electric effect [30]) however, only a full quantized theory is able to distinguish between “classical” (*e.g.* coherent, thermal) and “non-classical” (*e.g.* Fock, squeezed) states of light [5, 6]. The Hanbury-Brown and Twiss [31] experiment that yielded the “photon bunching” effect for thermal light is expected to show *anti-bunching* for Fock states of light, a completely non-classical effect. The first to prove the existence of such non-classical states of light were Kimble, Dagenais and Mandel [7].

Using a beam splitter and a source of parametric down-conversion, Hong, Ou and Mandel [9] experimentally proved the existence of this non-classical effect for pairs of single-quantum light states. Varying the arrival time of the “single photon wave packets” they obtained what we now call the “HOM dip”: a sharp drop in the coincidence counts when the light quanta impinge simultaneously on the beam splitter. Other variants of this experiment exist, for example with independent light sources [32, 33].

The question if the localized “photon wave packets” impinging simultaneously on the beam splitter tell the whole story arose ever since the HOM experiment. In order to answer this question, Pittman *et al.* [34] performed the same HOM interferometer experiment but with a voluntary time delay between the “photon wave packets” at the beam splitter, compensated thereafter before the detectors. The same dip was obtained in the coincidence counting rate, thus proving that the reassuring image of overlapping “photon wave packets” at the beam splitter is not the key to this experiment and the authors conclude that “the intuitively comforting notion of the photons overlapping at the beam splitter is not at the heart of the interference, but a mere artifact of the particular geometry of the setups” [34]. Kim *et al.* [35] and later Kim [36] went even further, proving that separating the “single photon pulses” beyond the coherence time of the pump laser still yields the famous HOM dip, with a visibility of more than 80%. The initial experiment (without delays) was also performed with orthogonal polarizations imposed to its input (*i.e.* $|V\rangle$ and $|H\rangle$). As expected, no interference was found, although the “photon wave packets” overlap at the beam splitter. The author concludes that “[...] the photon bunching picture often used in literature is indeed incorrect in general and should not be

*Electronic address: ataman@ece.fr

used whenever possible”.

Bylander *et al.* [37], using single light quanta from different sources in successive pulses show that the same phenomenon takes place, if indistinguishability is assured.

It is often believed that only identical (*i.e.* having the same energy) single-quantum states of light can produce this type of HOM interference. Indistinguishability [38] is indeed, important, but on the detector side. Raymer *et al.* [39] propose an interference experiment of “two photons of different color”. Using an active beam splitter, the initially distinguishable “red” and “blue” single-photon states can be converted into indistinguishable “green” single-photon states, hence the quantum interference leading to the HOM dip.

In spite of all these experiments, the localized “photon wave packet” picture is widely found today in literature, giving the impression that it is an unquestionable common place knowledge. We can read such statements as “the length of the photon wave packet”, “the photon wave packets overlap” or “the photons were short”, and we can even see graphics depicting Gaussian-damped sinusoids impinging on a beam splitter or on a detector, thus giving the impression that the very localized photon wave packet is taken more or less seriously.

We wish to add another argument in this paper in order to dispel this simplistic view of light quanta impinging on a beam splitter. However, compared to previous experiments, we propose a simple setup, requiring only photon pair production (from a parametric down-conversion source, for example), photo-detectors and regular beam splitters. No polarization beam splitters and no expensive pulse creation/selection equipment is required.

This paper is organized as follows. In Section II we describe in the formalism of Quantum Optics the beam-splitter and the Mach-Zehnder interferometer. We discuss the anti-bunching effect of a beam-splitter in Section III. The quantum-optical description of a double MZI experiment is done in Section IV. Two experiments with the double MZI experiment are proposed: in Section V the experimental setup is excited with a single-quantum Fock state while singles probability counts are evaluated and in Section VI two single-quantum states impinge simultaneously at its input while the main focus lies on the coincidence photo-counts. Finally, conclusions are drawn in Section VII.

II. THE QUANTUM OPTICAL DESCRIPTION OF BEAM SPLITTERS AND MACH-ZEHNDER INTERFEROMETERS

In the following we shall denote by \hat{a}_k (\hat{a}_k^\dagger) and, respectively, $\hat{D}_k(\alpha)$, the annihilation (creation) and, respectively, displacement operators acting at the port k . The quantum state of light $|\phi\rangle = |1_0 0_1\rangle$ denotes a state with one quantum of light in mode (port) 0 and none in mode (port) 1. Throughout this paper, all photo-detectors are

assumed to be ideal.

A. The case of monochromatic light

For a lossless beam splitter, the output annihilation operators (\hat{a}_3 and \hat{a}_2) can be written in respect with the input field operators [1] as

$$\hat{a}_3 = T\hat{a}_1 + R\hat{a}_0 \quad (1)$$

and

$$\hat{a}_2 = R\hat{a}_1 + T\hat{a}_0 \quad (2)$$

where T and R represent the transmission, and, respectively, the reflection coefficients. The input field operators (\hat{a}_0 and \hat{a}_1) obey the usual commutation relations $[\hat{a}_l, \hat{a}_k] = [\hat{a}_l^\dagger, \hat{a}_k^\dagger] = 0$ and $[\hat{a}_l, \hat{a}_k^\dagger] = \delta_{lk}$ where δ_{lk} is the Kronecker delta and $l, k = 0, 1$. We impose the same commutation relations to the output field operators and end up with the constraints

$$|T|^2 + |R|^2 = 1 \quad (3)$$

and

$$RT^* + TR^* = 0 \quad (4)$$

At this point we have the freedom to choose the phase of our coefficients. When dealing with a balanced (50/50) beam splitter, we shall use $T = 1/\sqrt{2}$ and $R = i/\sqrt{2}$ [1, 4]. From Eqs. (1) and (2) one can also obtain the “inverse” relations involving creation operators,

$$\hat{a}_0^\dagger = T\hat{a}_2^\dagger + R\hat{a}_3^\dagger \quad (5)$$

and

$$\hat{a}_1^\dagger = R\hat{a}_2^\dagger + T\hat{a}_3^\dagger \quad (6)$$

It is interesting to compare the output of a BS when at its input one applies a single-quantum Fock state and, respectively, a coherent state. In the first case we have $|\psi_{in}\rangle = \hat{a}_1^\dagger|0\rangle$, therefore

$$|\psi_{out}\rangle = R|1_2 0_3\rangle + T|0_2 1_3\rangle \quad (7)$$

This is an *entangled state* and detecting separately photons in any of the output ports will simply yield a probability of $|R|^2$ or $|T|^2$. However, the probability of coincident counts at its output yields

$$P_c = \langle \psi_{out} | \hat{a}_2^\dagger \hat{a}_3^\dagger \hat{a}_3 \hat{a}_2 | \psi_{out} \rangle = 0 \quad (8)$$

a result that is expected since we have a single quantum state that cannot yield multiple detections. In the second case, we describe the coherent state using the displacement operator relation $\hat{D}_1(\alpha) = \hat{D}_2(R\alpha) \hat{D}_3(T\alpha)$ [1, 4] and we find

$$|\psi_{out}\rangle = \hat{D}_2(R\alpha) \hat{D}_3(T\alpha) |0\rangle = |(R\alpha)_2 (T\alpha)_3\rangle \quad (9)$$

yielding a *non-entangled state*, fundamentally different from a state given by Eq. (7). Even for very small α , such a state will yield a non-null coincidence rate, as proven in the experiment of Aspect and Grangier [6].

Another interesting state at the input of a beam splitter would be $|\psi_{in}\rangle = R|0_01_1\rangle + T|1_00_1\rangle$. Using Eqs. (5) and (6), we find the output state

$$|\psi_{out}\rangle = 2RT|1_20_3\rangle + (R^2 + T^2)|0_21_3\rangle \quad (10)$$

and in the case of a balanced beam splitter we have $R^2 + T^2 = 0$, therefore $|\psi_{out}\rangle = |1_20_3\rangle$. In this case, the beam splitter transforms an *entangled state* into a *non-entangled* one, where the light quantum always leaves the beam splitter from the same port.

In the following (except when specifically stated) we will assume *balanced* (50/50) beam splitters.

The Mach-Zehnder interferometer (depicted in Fig. 1) is composed of two mirrors and two beam splitters. The delay φ_1 models the difference in optical path lengths between the two arms of the interferometer. For monochromatic light quanta of frequency ω we can write $\varphi_1 = \omega\tau_1$ where τ_1 denotes the time delay introduced. We can relate it to z , the path length difference of the MZI and we obviously have $\tau_1 = z/c$ where c is the speed of light in vacuum. The input creation operators in respect with the output ones are obtained from Eqs. (5) and (6), applied to both beam splitters. Combining them and considering the delay φ_1 applied to \hat{a}_3^\dagger , we end up with

$$\hat{a}_0^\dagger = -\sin(\varphi_1/2)\hat{a}_4^\dagger + \cos(\varphi_1/2)\hat{a}_5^\dagger \quad (11)$$

and

$$\hat{a}_1^\dagger = \cos(\varphi_1/2)\hat{a}_4^\dagger + \sin(\varphi_1/2)\hat{a}_5^\dagger \quad (12)$$

A single-quantum Fock state $|\psi_{in}\rangle = |0_01_1\rangle$ applied to the MZI is transformed into

$$|\psi_{out}\rangle = \cos(\varphi_1/2)|0_51_4\rangle + \sin(\varphi_1/2)|0_41_5\rangle \quad (13)$$

yielding the well-known sine-like probability of singles detection,

$$P_4 = |\langle 1_40_5|\psi_{out}\rangle|^2 = \frac{1}{2}(1 + \cos(\omega\tau_1)) \quad (14)$$

and

$$P_5 = |\langle 0_41_5|\psi_{out}\rangle|^2 = \frac{1}{2}(1 - \cos(\omega\tau_1)) \quad (15)$$

in respect with $\varphi_1 = \omega\tau_1$. A more interesting situation appears if we apply two simultaneously impinging light quanta on the first beam splitter *i.e.* $|\psi_{in}\rangle = |1_01_1\rangle$. This time, we have the output state

$$\begin{aligned} |\psi_{out}\rangle = & -1/\sqrt{2}\sin(\varphi_1)|2_40_5\rangle \\ & +1/\sqrt{2}\sin(\varphi_1)|0_42_5\rangle + \cos(\varphi_1)|1_41_5\rangle \end{aligned} \quad (16)$$

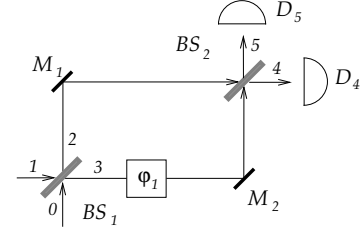


FIG. 1: A Mach-Zehnder interferometer. The delay φ_1 models the difference in optical path lengths between the two arms of the interferometer. D_4 and D_5 denote the photo-detectors placed at the two outputs of beam splitter BS_2 .

The probability of coincident detections at D_4 and D_5 is given by

$$P_c = |\langle 1_41_5|\psi_{out}\rangle|^2 = \frac{1}{2}(1 + \cos(2\varphi_1)) \quad (17)$$

showing that indeed, by continuously varying φ_1 the coincidence probability P_c goes back and forth between 0 to 1. For $\varphi_1 = 0$ we have $|1_01_1\rangle \rightarrow |1_41_5\rangle$, or, in other words, the MZI is *transparent* to the $|1_01_1\rangle$ input state.

It is worthwhile to note that in Eq. (17) the frequency of variation of the interference fringes is twice the frequency of the input light source. This phenomenon was experimentally tested by Rarity *et al.* [19]. They used pairs of correlated light quanta from a $\lambda = 826.8$ nm source obtained from down-converting a 413.4 nm krypton-ion laser. They found that the spatial period of the probability coincidence corresponds to the 413 nm of the pump laser.

B. The case of non-monochromatic light

Extension to a continuum of modes has been already considered [1, 40], often for two-photon states impinging on a beam splitter [32, 41]. Assuming non-monochromatic but *narrowband* light quanta, Legero *et al.* [42, 43] extend the result from Eq. (26) with a space-time domain description by considering spatio-temporal mode functions $\zeta_l(z, t) = \epsilon_l(t - z/c)e^{-i\phi_l(t - z/c)}$ of a single-mode input radiation (input ports are labelled $l = 0$ and $l = 1$). By placing the beam-splitter at $z = 0$ the space coordinate z can be omitted. The mode functions are assumed to be normalized, so that $\int |\epsilon_l(t)|^2 dt = 1$. Then, the input electric field operators can be written as $\hat{E}_l^{(+)}(t) = \zeta_l(t)\hat{a}_l$ and $\hat{E}_l^{(-)}(t) = \zeta_l^*(t)\hat{a}_l^\dagger$ with $l = 0, 1$ while the output electric fields are

$$\hat{E}_2^{(+)}(t) = \frac{1}{\sqrt{2}}(\zeta_0(t)\hat{a}_0 + i\zeta_1(t)\hat{a}_1) \quad (18)$$

and

$$\hat{E}_3^{(+)}(t) = \frac{1}{\sqrt{2}}(i\zeta_0(t)\hat{a}_0 + \zeta_1(t)\hat{a}_1) \quad (19)$$

The output field operators for the MZI are

$$\hat{E}_4^{(+)}(t) = \frac{\zeta_0(t) - \zeta_0(t - \tau_1)}{2} \hat{a}_0 + \frac{\zeta_1(t) + \zeta_1(t - \tau_1)}{2} i \hat{a}_1 \quad (20)$$

and

$$\hat{E}_5^{(+)}(t) = \frac{\zeta_0(t) + \zeta_0(t - \tau_1)}{2} i \hat{a}_0 - \frac{\zeta_1(t) - \zeta_1(t - \tau_1)}{2} \hat{a}_1 \quad (21)$$

If the input state $|\psi_{in}\rangle = |0_0 1_1\rangle$ is applied to our MZI, we find the probability of singles detection at D_4 given by

$$P_4 = \langle \psi_{in} | \hat{E}_4^{(-)}(t_0) \hat{E}_4^{(+)}(t_0) | \psi_{in} \rangle = \frac{1}{4} |\zeta_1(t_0) + \zeta_1(t_0 - \tau_1)|^2 \quad (22)$$

If we consider a Gaussian space-time mode function Eq. (30) for $\zeta_1(t)$, after t_0 -integration (a similar – slightly more complicated – computation is done in Appendix C) we arrive at

$$P_4 = \frac{1}{2} \left(1 + e^{-\frac{\tau_1^2}{\sigma^2}} \cos(\omega \tau_1) \right) \quad (23)$$

where this time ω represents the central frequency of our narrowband light quantum. We find the same oscillatory behavior from Eq. (14), however damped because of the finite bandwidth assumed for our light quantum. If we input the state $|\psi_{in}\rangle = |1_0 1_1\rangle$ to the MZI, one finds the probability of coincident counts

$$P_c(t_0, \tau, \tau_d) = \langle \psi_{in} | \hat{E}_4^{(-)}(t_0) \hat{E}_5^{(-)}(t_0 + \tau_d) \hat{E}_5^{(+)}(t_0 + \tau_d) \hat{E}_4^{(+)}(t_0) | \psi_{in} \rangle \quad (24)$$

where τ_d corresponds to the time delay between the detections at D_4 and D_5 , related to their distance from the beam splitter BS₂. If we set $\tau_d = 0$ in Eq. (24) and replace the functions $\zeta_0(t)$ and $\zeta_1(t)$ with the Gaussian expressions from Eqs. (29) and (30), after time integration one gets

$$P_c = \frac{1}{2} \left(1 + e^{-\frac{\tau_1^2}{\sigma^2}} \cos(2\omega \tau_1) \right) \quad (25)$$

where we find again the same oscillatory behavior from Eq. (17), damped however by an exponential factor.

III. THE ANTI-BUNCHING EFFECT ON A BEAM SPLITTER

A. The case of monochromatic light

We consider the input state $|\psi\rangle_{in} = |1_0 1_1\rangle$ *i.e.* two simultaneously impinging light quanta on a beam splitter with transmission (reflection) coefficient T (R). Using Eqs. (5) and (6), we obtain the output state

$$|\psi_{out}\rangle = \sqrt{2} (RT|0_2 2_3\rangle + RT|2_2 0_3\rangle) + (R^2 + T^2)|1_2 1_3\rangle \quad (26)$$

If the beam-splitter is balanced, we have $R^2 + T^2 = 0$, therefore the $|1_2 1_3\rangle$ output state from Eq. (26) vanishes. In other words, both light quanta will always exit the beam splitter through the same port. This is the *anti-bunching* or HOM effect.

B. The case of non-monochromatic light

The input state is still assumed to be $|\psi_{in}\rangle = |1_0 1_1\rangle$. The non-monochromatic character of the light quanta will be modelled through the field operators $\hat{E}_2^{(+)}(t)$ and $\hat{E}_3^{(+)}(t)$. The probability of joint detection at the outputs of the beam splitter at times t_0 and, respectively $t_0 + \tau_d$ is

$$P_c(t_0, \tau_d) = \langle \psi_{in} | \hat{E}_2^{(-)}(t_0) \hat{E}_3^{(-)}(t_0 + \tau_d) \hat{E}_3^{(+)}(t_0 + \tau_d) \hat{E}_2^{(+)}(t_0) | \psi_{in} \rangle \quad (27)$$

and after a series of calculations [42, 43] the final result reads

$$P_c(t_0, \tau_d) = \frac{1}{4} |\zeta_0(t_0 + \tau_d) \zeta_1(t_0) - \zeta_0(t_0) \zeta_1(t_0 + \tau_d)|^2 \quad (28)$$

implying that indeed, for simultaneously impinging light quanta on the beam splitter, detected at the same time ($\tau_d = 0$), the probability of coincident counts is $P_c = 0$, regardless of the temporal shapes of $\zeta_0(t)$ and $\zeta_1(t)$. We can take Gaussian spatio-temporal mode functions,

$$\zeta_0(t) = \left(\frac{2}{\pi \sigma^2} \right)^{\frac{1}{4}} e^{-\frac{(t - \tau_e/2)^2}{\sigma^2} - i\omega t} \quad (29)$$

and

$$\zeta_1(t) = \left(\frac{2}{\pi \sigma^2} \right)^{\frac{1}{4}} e^{-\frac{(t + \tau_e/2)^2}{\sigma^2} - i\omega t} \quad (30)$$

where σ quantifies the time spread of our light quanta and τ_e can be seen as the time difference of the impinging Gaussian “photon wave packets” on the beam splitter. The probability of coincident counts from Eq. (28) is easily evaluated to

$$P_c(t_0, \tau_e, \tau_d) = \frac{\cosh(2\tau_d \tau_e / \sigma^2) - 1}{\pi \sigma^2} e^{-\frac{4t_0(t_0 + \tau_d) + \tau_e^2 + 2\tau_d^2}{\sigma^2}} \quad (31)$$

and integrating it over all possible values of t_0 we get

$$P_c(\tau_e, \tau_d) = \frac{\cosh(2\tau_d \tau_e / \sigma^2) - 1}{2\sqrt{\pi} \sigma} e^{-\frac{\tau_e^2 + \tau_d^2}{\sigma^2}} \quad (32)$$

If the photo-detectors are “slow”, we integrate $P_c(\tau_e, \tau_d)$ over the detection time difference τ_d , yielding

$$P_c(\tau_e) = \frac{1}{2} \left(1 - e^{-\frac{\tau_e^2}{\sigma^2}} \right) \quad (33)$$

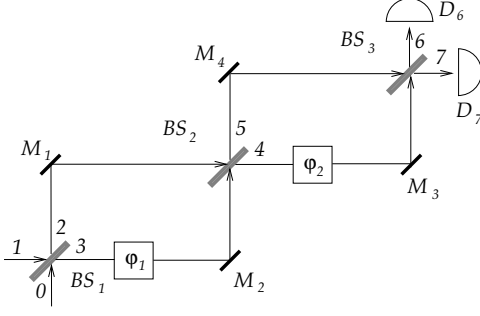


FIG. 2: The double MZI experiment proposed in Section IV. The first MZI is composed of the beam splitters BS_1 and BS_2 together with the mirrors M_1 and M_2 . Similarly, the second MZI is composed of BS_2 , BS_3 , M_3 and M_4 . φ_1 and, respectively φ_2 represent delays voluntarily introduced in the paths labelled “3” and, respectively, “4”.

This detection probability shows indeed the very famous “HOM dip”, experimentally measured by Hong, Ou and Mandel [9], where they report a time measurement of a “sub-picosecond photon wave packet”. The fact that those “photon wave packets” meet at the beam splitter seems to cause the famous dip in the rate of coincidences at the detector. Eq. (33) quantifies this result, implying that a null coincidence probability can only be achieved if $\tau_e = 0$ *i.e.* if both “photon wave packets” are impinging simultaneously on the beam splitter.

IV. THE QUANTUM OPTICAL DESCRIPTION OF A DOUBLE MZI EXPERIMENT

In the following, we introduce and discuss a double MZI interferometer experiment (depicted in Fig. 2). The beam splitter BS_1 , together with the beam splitter BS_2 and the two mirrors M_1 and M_2 form the first MZI. In the lower path a delay φ_1 is introduced. The second MZI is composed of the beam splitters BS_2 and BS_3 , together with the two corresponding mirrors M_3 and M_4 . In the lower path of this interferometer a delay φ_2 is present. It is assumed that, with the corresponding delays taken out of the experiment, each MZI has equal length arms. Photo-detectors D_6 and D_7 are installed at the two outputs of BS_3 .

A. The case of monochromatic light

The input (creation) field operators (ignoring some common phase factors) in respect with the output field operators are (see Appendix A)

$$\hat{a}_0^\dagger = \frac{-i \sin\left(\frac{\varphi_2}{2}\right) - e^{-i\varphi_1} \cos\left(\frac{\varphi_2}{2}\right)}{\sqrt{2}} \hat{a}_6^\dagger + \frac{i \cos\left(\frac{\varphi_2}{2}\right) - e^{-i\varphi_1} \sin\left(\frac{\varphi_2}{2}\right)}{\sqrt{2}} \hat{a}_7^\dagger \quad (34)$$

and

$$\hat{a}_1^\dagger = \frac{\sin\left(\frac{\varphi_2}{2}\right) + ie^{-i\varphi_1} \cos\left(\frac{\varphi_2}{2}\right)}{\sqrt{2}} \hat{a}_6^\dagger + \frac{-\cos\left(\frac{\varphi_2}{2}\right) + ie^{-i\varphi_1} \sin\left(\frac{\varphi_2}{2}\right)}{\sqrt{2}} \hat{a}_7^\dagger \quad (35)$$

These relations will be used in the next sections in order to compute the output state of our system.

B. The case of non-monochromatic light

The output field operators $\hat{E}_6^{(+)}(t)$ and $\hat{E}_7^{(+)}(t)$ expressed in respect with the input fields are (see details in Appendix B)

$$\hat{E}_6^{(+)}(t) = \frac{1}{2\sqrt{2}} \left(\hat{a}_0(\zeta_0(t - \tau_2) - \zeta_0(t - \tau_1 - \tau_2)) - \zeta_0(t) - \zeta_0(t - \tau_1) \right) + i\hat{a}_1(\zeta_1(t - \tau_2) + \zeta_1(t - \tau_1 - \tau_2) - \zeta_1(t) + \zeta_1(t - \tau_1)) \quad (36)$$

and

$$\hat{E}_7^{(+)}(t) = \frac{1}{2\sqrt{2}} \left(i\hat{a}_0(\zeta_0(t - \tau_2) - \zeta_0(t - \tau_1 - \tau_2)) + \zeta_0(t) + \zeta_0(t - \tau_1) \right) + \hat{a}_1(-\zeta_1(t - \tau_2) - \zeta_1(t - \tau_1 - \tau_2) - \zeta_1(t) + \zeta_1(t - \tau_1)) \quad (37)$$

We obviously have $\hat{E}_6^{(-)}(t) = [\hat{E}_6^{(+)}(t)]^\dagger$ and $\hat{E}_7^{(-)}(t) = [\hat{E}_7^{(+)}(t)]^\dagger$. These field operators will be used in the next sections in order to find singles and coincidence photo-detection probabilities.

V. THE DOUBLE MZI WITH A SINGLE LIGHT QUANTUM AT ONE INPUT

In this section we analyze the double MZI experimental setup when at its input we have a single quantum (monochromatic or non-monochromatic) Fock state.

A. The case of monochromatic light

The input state can be written as $|\psi_{in}\rangle = \hat{a}_1^\dagger|0\rangle$ and taking into account Eq. (35) we have

$$|\psi_{out}\rangle = \frac{\sin\left(\frac{\varphi_2}{2}\right) + ie^{-i\varphi_1} \cos\left(\frac{\varphi_2}{2}\right)}{\sqrt{2}} |1_6 0_7\rangle + \frac{-\cos\left(\frac{\varphi_2}{2}\right) + ie^{-i\varphi_1} \sin\left(\frac{\varphi_2}{2}\right)}{\sqrt{2}} |0_6 1_7\rangle \quad (38)$$

The probability of single-photon detection at the detector D_6 can be easily computed, yielding

$$P_6 = | \langle 1_6 0_7 | \psi_{out} \rangle |^2 = \frac{1}{2} \left(1 + \sin(\varphi_1) \sin(\varphi_2) \right) \quad (39)$$

Similarly, computing the single-photon detection probability at the detector D_7 we find

$$P_7 = |\langle 0_6 1_7 | \psi_{out} \rangle|^2 = \frac{1}{2} \left(1 - \sin(\varphi_1) \sin(\varphi_2) \right) \quad (40)$$

and we have $P_6 + P_7 = 1$, as expected. However, Eqs. (39) and (40) imply that the sine-like variation of the detection probabilities in respect with the length difference of the two arms for a single MZI (as found in Section II A) is no longer true. Indeed, by setting for example $\sin(\varphi_1) = 0$, we end up with $P_6 = P_7 = 1/2$, no matter what value φ_2 takes. The same is true for φ_1 if we fix $\sin(\varphi_2) = 0$.

This apparent paradox of Eqs. (39) and (40) can be explained if we consider, for example, the state of the field at the output of beam splitter BS_2 for $\sin \varphi_1 = 0$. Indeed, using Eq. (10) we find $|\psi_{45}\rangle = |0_5 1_4\rangle$. In other words, our light quantum *always takes only one arm* in the second MZI. The delay φ_2 becomes therefore, useless.

If we set φ_1 so that we have $\sin(\varphi_1) = \beta$, the probability of single-photon detection at the detector D_6 will be $P_6 = 1/2 (1 + \beta \sin(\varphi_2))$, in other words, the delay φ_1 modulates the photo-detection probability $P_6(\varphi_2)$.

The probability of coincident counts is $P_c = 0$, an expected result since a single light quantum cannot yield multiple output detections. However if we apply a coherent source instead of the Fock state, the situation dramatically changes. Indeed, for a state $|\psi_{in}\rangle = |0_0 \alpha_1\rangle$ we find

$$|\psi_{out}\rangle = \hat{D}_6 \left(\alpha \frac{\sin(\varphi_2/2) + ie^{-i\varphi_1} \cos(\varphi_2/2)}{\sqrt{2}} \right) \hat{D}_7 \left(\alpha \frac{-\cos(\frac{\varphi_2}{2}) + ie^{-i\varphi_1} \sin(\frac{\varphi_2}{2})}{\sqrt{2}} \right) |0\rangle \quad (41)$$

The rate of coincidence detection is proportional to

$$N_c \sim \frac{|\alpha|^4}{4} \left(1 - \sin^2(\varphi_1) \sin^2(\varphi_2) \right) \quad (42)$$

For the singles rates one easily finds

$$N_6 \sim \frac{|\alpha|^2}{2} \left(1 + \sin(\varphi_1) \sin(\varphi_2) \right) \quad (43)$$

and

$$N_7 \sim \frac{|\alpha|^2}{2} \left(1 - \sin(\varphi_1) \sin(\varphi_2) \right) \quad (44)$$

implying $N_c/N_6 N_7 = 1$ *i.e.* we have *no antibunching* with a coherent state.

B. The case of non-monochromatic light

If we suppose a single light quantum having some spatio-temporal extension $\zeta_1(t)$, we characterize the probability of single-photon detection at time t_0 at the detector D_6 by

$$P_6 = \langle \psi_{in} | \hat{E}_6^-(t_0) \hat{E}_6^+(t_0) | \psi_{in} \rangle \quad (45)$$

Using Eq. (36), replacing the Gaussian waveforms and time-integrating the result (see details in Appendix C) takes us to

$$P_6 = \frac{1}{4} \left(2 + e^{-\frac{(\tau_1 - \tau_2)^2}{2\sigma^2}} \cos(\omega(\tau_1 - \tau_2)) - e^{-\frac{(\tau_1 + \tau_2)^2}{2\sigma^2}} \cos(\omega(\tau_1 + \tau_2)) \right) \quad (46)$$

Performing the same computations for the detector D_7 yields

$$P_7 = \frac{1}{4} \left(2 - e^{-\frac{(\tau_1 - \tau_2)^2}{2\sigma^2}} \cos(\omega(\tau_1 - \tau_2)) + e^{-\frac{(\tau_1 + \tau_2)^2}{2\sigma^2}} \cos(\omega(\tau_1 + \tau_2)) \right) \quad (47)$$

If we fix τ_1 so that $\sin(\omega\tau_1) = \beta$ and denoting $\kappa = \tau_1/\sigma^2$, $\gamma = \sqrt{1 - \beta^2} e^{-\tau_1^2/2\sigma^2}$ and $\delta = \beta e^{-\tau_1^2/2\sigma^2}$, we can rewrite the singles detection probabilities as

$$P_6 = \frac{1}{2} \left(1 - \gamma e^{-\frac{\tau_2^2}{2\sigma^2}} \sinh(\kappa\tau_2) \cos(\omega\tau_2) - \delta e^{-\frac{\tau_2^2}{2\sigma^2}} \cosh(\kappa\tau_2) \sin(\omega\tau_2) \right) \quad (48)$$

and

$$P_7 = \frac{1}{2} \left(1 + \gamma e^{-\frac{\tau_2^2}{2\sigma^2}} \sinh(\kappa\tau_2) \cos(\omega\tau_2) + \delta e^{-\frac{\tau_2^2}{2\sigma^2}} \cosh(\kappa\tau_2) \sin(\omega\tau_2) \right) \quad (49)$$

We depict in Fig. 3 P_6 and P_7 for three different values of β . This parameter β imposes constraints on the maximum amplitude of the sine-like behavior of the probabilities P_6 and P_7 while the Gaussian shaping causes them to “fade” towards the value of $1/2$ as τ_2 increases. For $\beta = 0$ we obviously have $P_6(\tau_2) = P_7(\tau_2) = 1/2$, whatever the value of τ_2 .

If we consider the transition to monochromatic light quanta (*i.e.* when $\sigma \rightarrow \infty$), it is easy to show that we obtain again P_6 and, respectively, P_7 given by Eqs. (39) and, respectively, (40).

VI. THE DOUBLE MZI WITH TWO SIMULTANEOUSLY IMPINGING LIGHT QUANTA AT ITS INPUTS

In this section we describe an experiment with the double MZI depicted Fig. 2, able to show that the antibunching effect on a beam splitter has nothing to do with “photon wave packets meeting at the beam splitter”. Both the monochromatic and the non-monochromatic cases are discussed.

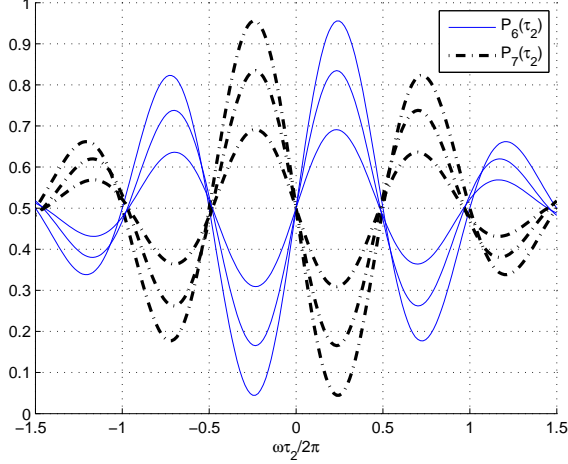


FIG. 3: The probability of single-photon detection for $P_6(\tau_2)$ and, respectively, $P_7(\tau_2)$ given by Eq. (48) and, respectively, Eq. (49) for $\beta = 1$ (highest amplitude curves), $\beta = 0.707$ and $\beta = 0.4$ (lowest amplitude curves). We used for this simulation $\sigma\omega = 5$.

A. The case of monochromatic light

With arbitrary delays φ_1 and φ_2 , for the input state $|\psi_{in}\rangle = |1_0 1_1\rangle$ by using Eqs. (34) and (35) one finds the output state

$$|\psi_{out}\rangle = \frac{\sin(\varphi_1) \cos(\varphi_2) - i \cos(\varphi_1)}{\sqrt{2}} |0_6 2_7\rangle - \frac{\sin(\varphi_1) \cos(\varphi_2) - i \cos(\varphi_1)}{\sqrt{2}} |2_6 0_7\rangle + \sin(\varphi_1) \sin(\varphi_2) |1_6 1_7\rangle \quad (50)$$

The probability of coincident detections at the outputs detectors D_6 and D_7 is given by

$$P_c(\varphi_1, \varphi_2) = |\langle 1_6 1_7 | \psi_{out} \rangle|^2 = \sin^2(\varphi_1) \sin^2(\varphi_2) \quad (51)$$

If we take out both delays from the experimental setup, we end up with the same type of transformation given by Eq. (26) *i.e.* the whole experiment is equivalent to a *beam splitter*. At this point we can claim that the “photon wave packets” meet at the beam splitter BS_2 . However, the same transformation can be obtained with the delays in place, by choosing $\varphi_1 = \varphi_2 = m\pi$ where $m \in \mathbb{N}^*$. These delays can be made arbitrarily large, the only limitation being imposed by the coherence properties of the light source. This way, the output state from (50) becomes

$$|\psi_{out}\rangle = -\frac{i}{\sqrt{2}} |0_6 2_7\rangle + \frac{i}{\sqrt{2}} |2_6 0_7\rangle \quad (52)$$

i.e. a perfect anti-correlation that we expect to show the famous “HOM dip” in the case of non-monochromatic light quanta. However, this time we have no possible

way of having “overlapping photon wave packets” at the beam splitter¹ BS_2 .

This experiment can also be seen as a delayed “photon wave packets” HOM interferometer at the beam splitter BS_2 while the two other beam splitters act as quantum erasers, so that the interfering paths at BS_2 become indiscernible.

B. The case of non-monochromatic light

Extending the above results to spatio-temporal modes, the probability of coincident counts at detectors D_6 and D_7 , at times t_0 and, respectively, $t_0 + \tau_d$ is given by

$$P_c(t_0, \tau_1, \tau_2, \tau_d) = \langle \psi_{in} | \hat{E}_6^{(-)}(t_0) \hat{E}_7^{(-)}(t_0 + \tau_d) \hat{E}_7^{(+)}(t_0 + \tau_d) \hat{E}_6^{(+)}(t_0) | \psi_{in} \rangle \quad (53)$$

We will be interested in the time-integrated detection probability over all t_0 and, eventually, for the non time-resolved detection, integrated over τ_d , also.

The general form of the probability of coincident counts is rather complicated, but if we restrict to $\tau_d = 0$, Eq. (53) simplifies to (see details in Appendix D)

$$P_c(t_0, \tau_1, \tau_2) = \frac{1}{16} \left| [\zeta_0(t_0) + \zeta_0(t_0 - \tau_1)] \cdot [\zeta_1(t_0) - \zeta_1(t_0 - \tau_1)] - [\zeta_0(t_0 - \tau_2) - \zeta_0(t_0 - \tau_1 - \tau_2)] \cdot [\zeta_1(t_0 - \tau_2) + \zeta_1(t_0 - \tau_1 - \tau_2)] \right|^2 \quad (54)$$

If we employ the spatio-temporal modes from Eqs. (29) and (30), after a series of rather long calculations (detailed in Appendix E), the time-integrated (over t_0 and τ_d) probability of coincidence for $\tau_e = 0$ yields

$$P_c(\tau_1, \tau_2) = \frac{1}{8} \left(2 - 2e^{-\frac{\tau_1^2}{\sigma^2}} \cos(2\omega\tau_1) - 2e^{-\frac{\tau_2^2}{\sigma^2}} \cos(2\omega\tau_2) + e^{-\frac{(\tau_1 + \tau_2)^2}{\sigma^2}} \cos(2\omega(\tau_1 + \tau_2)) + e^{-\frac{(\tau_1 - \tau_2)^2}{\sigma^2}} \cos(2\omega(\tau_1 - \tau_2)) \right) \quad (55)$$

The surface plot of P_c from Eq. (55) versus τ_1 and τ_2 is depicted in Fig. 4. As expected, for $\tau_1 = \tau_2 = 0$, we have a dip in the probability of coincident counts. But besides this dip, there are other minima of P_c for $\tau_1 \neq 0$ and $\tau_2 \neq 0$. This time, we have no possible “photon wave packets” overlapping at the beam splitter BS_2 .

¹ Strictly speaking, this experiment performs exactly the opposite of Eq. (26), namely we have $i/\sqrt{2}|0_2 2_3\rangle - i/\sqrt{2}|2_2 0_3\rangle \rightarrow |1_4 1_5\rangle$, which is, of course, perfectly equivalent to Eq. (26). But if we insist on finding exactly the anti-bunching effect from Eq. (26) at BS_2 , all we have to do is add another MZI in front of the first one.

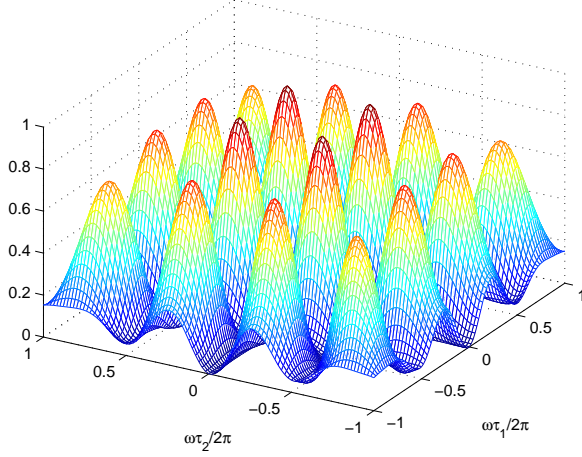


FIG. 4: The probability of coincident counts $P_c(\tau_1, \tau_2)$ given by Eq. (55) at the detectors D_6 and D_7 . The presence of multiple dips shows that the same behavior can be obtained with or without “overlapping photon wave packets” at the beam splitter BS₂. For this simulation we used $\sigma\omega = 7$ and $\tau_l\omega \in [-2\pi, 2\pi]$ with $l = 1, 2$.

If we consider the transition from narrowband to monochromatic light quanta (*i.e.* when $\sigma \rightarrow \infty$), Eq. (55) becomes $P_c(\tau_1, \tau_2) = \sin^2(\omega\tau_1) \sin^2(\omega\tau_2)$, *i.e.* we find the same result from Eq. (51).

VII. CONCLUSIONS

In this paper we introduced and analyzed a new experimental setup within the standard formalism of QO. The proposed double Mach-Zehnder interferometer experiment shows a counter-intuitive behavior when excited with a single light quantum: the path length difference of one MZI “modulates” the amplitude of singles detection rates versus the path length difference of the other MZI. In the extreme case, for certain values of the path length difference of one MZI, the output singles detection rates do not change, whatever the length of the other MZI.

In the case of two simultaneously impinging light quanta at its input, the double MZI experiment is able to show the same “HOM dip” behavior for certain values of the delays φ_1 and φ_2 , whether or not the “photon wave packets” meet at the second beam splitter. In the extreme case of nearly monochromatic light, φ_1 and φ_2 may introduce arbitrarily large delays, nonetheless the “HOM dip” in the coincident counts will be present, showing that the intuitive image of “overlapping photon wave packets” at the beam splitter has a questionable physical reality, not being the key to explain this experiment.

Appendix A: Computation of the input field operators in respect with the output ones

We write down the “inverse” input-output operator relations for each beam splitter. Starting with BS₁ we have

$$\hat{a}_1^\dagger = \frac{1}{\sqrt{2}} \left(i\hat{a}_2^\dagger + \hat{a}_3^\dagger \right) \quad (\text{A1})$$

and

$$\hat{a}_0^\dagger = \frac{1}{\sqrt{2}} \left(\hat{a}_2^\dagger + i\hat{a}_3^\dagger \right) \quad (\text{A2})$$

For the second beam splitter we also take into account the delay φ_1 , yielding

$$\hat{a}_2^\dagger = \frac{1}{\sqrt{2}} \left(\hat{a}_4^\dagger + i\hat{a}_5^\dagger \right) \quad (\text{A3})$$

and

$$\hat{a}_3^\dagger = e^{-i\varphi_1} \frac{1}{\sqrt{2}} \left(i\hat{a}_4^\dagger + \hat{a}_5^\dagger \right) \quad (\text{A4})$$

Finally, the beam splitter BS₃ transforms the field operators

$$\hat{a}_5^\dagger = \frac{1}{\sqrt{2}} \left(i\hat{a}_6^\dagger + \hat{a}_7^\dagger \right) \quad (\text{A5})$$

and

$$\hat{a}_4^\dagger = e^{-i\varphi_2} \frac{1}{\sqrt{2}} \left(\hat{a}_6^\dagger + i\hat{a}_7^\dagger \right) \quad (\text{A6})$$

where in the last equation we took into account the delay introduced by φ_2 . Combining Eqs. (A3) and (A4) into Eq. (A2), we obtain

$$\hat{a}_0^\dagger = \frac{1}{2} \left((1 - e^{-i\varphi_1}) \hat{a}_4^\dagger + i(1 + e^{-i\varphi_1}) \hat{a}_5^\dagger \right) \quad (\text{A7})$$

and replacing \hat{a}_4^\dagger and \hat{a}_5^\dagger from (A5) and, respectively, (A6) yields

$$\begin{aligned} \hat{a}_0^\dagger = \frac{1}{2\sqrt{2}} & \left((1 - e^{-i\varphi_1}) e^{-i\varphi_2} (\hat{a}_6^\dagger + i\hat{a}_7^\dagger) \right. \\ & \left. + i(1 + e^{-i\varphi_1}) (i\hat{a}_6^\dagger + \hat{a}_7^\dagger) \right) \end{aligned} \quad (\text{A8})$$

We group together the \hat{a}_6^\dagger and \hat{a}_7^\dagger terms, arriving at the final expression

$$\begin{aligned} \hat{a}_0^\dagger = & \frac{e^{-i\varphi_2} - e^{-i\varphi_1}e^{-i\varphi_2} - 1 - e^{-i\varphi_1}}{2\sqrt{2}} \hat{a}_6^\dagger \\ & + \frac{e^{-i\varphi_2} - e^{-i\varphi_1}e^{-i\varphi_2} + 1 + e^{-i\varphi_1}}{2\sqrt{2}} i\hat{a}_7^\dagger \end{aligned} \quad (\text{A9})$$

Factoring out a common phase factor and replacing the complex exponentials with trigonometric functions takes

us to Eq. (34). Similar computations lead us to

$$\hat{a}_1^\dagger = \frac{e^{-i\varphi_2} + e^{-i\varphi_1}e^{-i\varphi_2} - 1 + e^{-i\varphi_1}}{2\sqrt{2}}i\hat{a}_6^\dagger + \frac{-e^{-i\varphi_2} - e^{-i\varphi_1}e^{-i\varphi_2} - 1 + e^{-i\varphi_1}}{2\sqrt{2}}\hat{a}_7^\dagger \quad (\text{A10})$$

and by the same factorization we end up with Eq. (35). Please note that in Eqs. (34) and (35) we chose to factor out φ_2 (*i.e.* we ended up with expressions involving sines and cosines of φ_2). The same operations could have been done with φ_1 . It can be shown that none of the observables (*e.g.* singles, coincidence detection rates etc.) changes.

Appendix B: Computation of the output field operators $\hat{E}_6^{(+)}(t)$ and $\hat{E}_7^{(+)}(t)$ for the double MZI experiment

We will deduce only the field operator $\hat{E}_7^{(+)}(t)$ since the computation for $\hat{E}_6^{(+)}(t)$ is following a similar path. We start with the beam splitter BS₃ and the output field operator $\hat{E}_7^{(+)}(t)$, connected to the input field operators by

$$\hat{E}_7^{(+)}(t) = \frac{1}{\sqrt{2}} \left(i\hat{E}_4^{(+)}(t - \tau_2) + \hat{E}_5^{(+)}(t) \right) \quad (\text{B1})$$

where in the first term we took into account the delay φ_2 . We replace now the field operators for the beam splitter BS₂, yielding

$$\hat{E}_4^{(+)}(t) = \frac{1}{\sqrt{2}} \left(\hat{E}_2^{(+)}(t) + i\hat{E}_3^{(+)}(t) \right) \quad (\text{B2})$$

and

$$\hat{E}_5^{(+)}(t) = \frac{1}{\sqrt{2}} \left(i\hat{E}_2^{(+)}(t) + \hat{E}_3^{(+)}(t) \right) \quad (\text{B3})$$

We can replace now these operators into (B1) yielding for our field operator

$$\hat{E}_7^{(+)}(t) = \frac{1}{2} \left(i\hat{E}_2^{(+)}(t - \tau_2) - \hat{E}_3^{(+)}(t - \tau_1 - \tau_2) + i\hat{E}_2^{(+)}(t) + \hat{E}_3^{(+)}(t - \tau_1) \right) \quad (\text{B4})$$

where we took into account the delay φ_1 for the field operator $\hat{E}_3^{(+)}(t)$. Combining Eqs. (18) and (19) with Eq. (B4), by simply regrouping some terms we arrive at the desired result Eq. (37).

Appendix C: Computation of the probability of singles detection for the double MZI experiment

For an input state $|\psi_{in}\rangle = |0_0 1_1\rangle = \hat{a}_1^\dagger|0\rangle$, the probability of photo-detection at the detector \bar{D}_6 can be written as

$$P_6 = \|\hat{E}_6^+(t_0)\hat{a}_1^\dagger|0\rangle\|^2 \quad (\text{C1})$$

This expression can be simplified if we note that only terms containing \hat{a}_1 will yield a contribution to P_6 since $\hat{a}_0\hat{a}_1^\dagger|0\rangle = 0$. Inserting Eq. (36) into Eq. (C1) leads to

$$P_6 = \frac{1}{8} \left| \zeta_1(t - \tau_2) + \zeta_1(t - \tau_1 - \tau_2) - \zeta_1(t) + \zeta_1(t - \tau_1) \right|^2 \quad (\text{C2})$$

We can replace now $\zeta_1(t)$ with the Gaussian mode defined in Eq. (30). Since τ_e has no meaning for a single light quantum, we set it to zero. Expanding the mod-square from Eq. (C2) yields

$$P_6 = \frac{1}{8} \sqrt{\frac{2}{\pi\sigma^2}} \left(e^{-2\frac{(t_0-\tau_2)^2}{\sigma^2}} + e^{-\frac{(t_0-\tau_2)^2}{\sigma^2}} e^{-\frac{(t_0-\tau_1-\tau_2)^2}{\sigma^2}} e^{-i\omega\tau_1} - e^{-\frac{(t_0-\tau_2)^2}{\sigma^2}} e^{-\frac{t_0^2}{\sigma^2}} e^{i\omega\tau_2} + e^{-\frac{(t_0-\tau_2)^2}{\sigma^2}} e^{-\frac{(t_0-\tau_1)^2}{\sigma^2}} e^{i\omega(\tau_2-\tau_1)} \right. \\ \left. + e^{-\frac{(t_0-\tau_1-\tau_2)^2}{\sigma^2}} e^{-\frac{(t_0-\tau_2)^2}{\sigma^2}} e^{i\omega\tau_1} + e^{-2\frac{(t_0-\tau_1-\tau_2)^2}{\sigma^2}} - e^{-\frac{(t_0-\tau_1-\tau_2)^2}{\sigma^2}} e^{-\frac{t_0^2}{\sigma^2}} e^{i\omega(\tau_1+\tau_2)} + e^{-\frac{(t_0-\tau_1-\tau_2)^2}{\sigma^2}} e^{-\frac{(t_0-\tau_1)^2}{\sigma^2}} e^{i\omega\tau_2} \right. \\ \left. - e^{-\frac{t_0^2}{\sigma^2}} e^{-\frac{(t_0-\tau_2)^2}{\sigma^2}} e^{-i\omega\tau_2} - e^{-\frac{t_0^2}{\sigma^2}} e^{-\frac{(t_0-\tau_1-\tau_2)^2}{\sigma^2}} e^{-i\omega(\tau_1+\tau_2)} + e^{-2\frac{t_0^2}{\sigma^2}} - e^{-\frac{t_0^2}{\sigma^2}} e^{-\frac{(t_0-\tau_1)^2}{\sigma^2}} e^{-i\omega\tau_1} \right. \\ \left. + e^{-\frac{(t_0-\tau_1)^2}{\sigma^2}} e^{-\frac{(t_0-\tau_2)^2}{\sigma^2}} e^{i\omega(\tau_1-\tau_2)} + e^{-\frac{(t_0-\tau_1)^2}{\sigma^2}} e^{-\frac{(t_0-\tau_1-\tau_2)^2}{\sigma^2}} e^{-i\omega\tau_2} - e^{-\frac{(t_0-\tau_1)^2}{\sigma^2}} e^{-\frac{t_0^2}{\sigma^2}} e^{i\omega\tau_1} + e^{-2\frac{(t_0-\tau_1)^2}{\sigma^2}} \right) \quad (\text{C3})$$

In order to t_0 -integrate the expression above we use the formula

$$\int_{-\infty}^{\infty} e^{-\frac{(y-a)^2}{\sigma^2}} e^{-\frac{(y-b)^2}{\sigma^2}} dy = \sqrt{\frac{\pi\sigma^2}{2}} e^{-\frac{(a-b)^2}{2\sigma^2}} \quad (\text{C4})$$

valid for any $a, b \in \mathbb{R}$ and $\sigma \in \mathbb{R}^*$. After time-integration and some simplifications we are left with

$$P_6 = \frac{1}{8} \left(4 + e^{-\frac{(\tau_1 - \tau_2)^2}{2\sigma^2}} e^{i\omega(\tau_2 - \tau_1)} + e^{-\frac{(\tau_1 - \tau_2)^2}{2\sigma^2}} e^{-i\omega(\tau_2 - \tau_1)} - e^{-\frac{(\tau_1 + \tau_2)^2}{2\sigma^2}} e^{i\omega(\tau_1 + \tau_2)} - e^{-\frac{(\tau_1 + \tau_2)^2}{2\sigma^2}} e^{-i\omega(\tau_1 + \tau_2)} \right) \quad (C5)$$

Grouping the complex exponentials into cosines takes us to the final result from Eq. (46). The computation of P_7 follows identical steps.

Appendix D: Computation of the probability of coincident counts for the double MZI experiment

The probability of coincident counts from Eq. (53) can be written as

$$P_c(t_0, \tau_1, \tau_2, \tau_d) = \|\hat{E}_7^{(+)}(t_0 + \tau_d) \hat{E}_6^{(+)}(t_0) \hat{a}_1^\dagger \hat{a}_0^\dagger |0\rangle\|^2 \quad (D1)$$

and we can readily discard from Eq. (D1) all terms containing \hat{a}_1^2 and \hat{a}_0^2 since $\hat{a}_1^2 \hat{a}_1^\dagger \hat{a}_0^\dagger |0\rangle = \hat{a}_0^2 \hat{a}_1^\dagger \hat{a}_0^\dagger |0\rangle = 0$. We are left with the rather complicated expression

$$\begin{aligned} P_c(t_0, \tau_1, \tau_2, \tau_d) = & \frac{1}{64} \left| \left(\zeta_0(t_0 - \tau_2) - \zeta_0(t_0 - \tau_1 - \tau_2) - \zeta_0(t_0) - \zeta_0(t_0 - \tau_1) \right) \right. \\ & \cdot \left(-\zeta_1(t_0 - \tau_2 + \tau_d) - \zeta_1(t_0 - \tau_1 - \tau_2 + \tau_d) - \zeta_1(t_0 + \tau_d) + \zeta_1(t_0 - \tau_1 + \tau_d) \right) \\ & - \left(\zeta_0(t_0 - \tau_2 + \tau_d) - \zeta_0(t_0 - \tau_1 - \tau_2 + \tau_d) + \zeta_0(t_0 + \tau_d) + \zeta_0(t_0 - \tau_1 + \tau_d) \right) \\ & \left. \cdot \left(\zeta_1(t_0 - \tau_2) + \zeta_1(t_0 - \tau_1 - \tau_2) - \zeta_1(t) + \zeta_1(t_0 - \tau_1) \right) \right|^2 \end{aligned} \quad (D2)$$

However, for $\tau_d = 0$ half of the terms disappear while the other half becomes pairs of identical terms yielding

$$\begin{aligned} P_c(t_0, \tau_1, \tau_2) = & \frac{1}{16} \left| -\zeta_0(t_0 - \tau_2) \zeta_1(t_0 - \tau_2) - \zeta_0(t_0 - \tau_2) \zeta_1(t_0 - \tau_1 - \tau_2) \right. \\ & + \zeta_0(t_0 - \tau_1 - \tau_2) \zeta_1(t_0 - \tau_2) + \zeta_0(t_0 - \tau_1 - \tau_2) \zeta_1(t_0 - \tau_1 - \tau_2) + \zeta_0(t_0) \zeta_1(t_0) \\ & \left. - \zeta_0(t_0) \zeta_1(t_0 - \tau_1) + \zeta_0(t_0 - \tau_1) \zeta_1(t_0) - \zeta_0(t_0 - \tau_1) \zeta_1(t_0 - \tau_1) \right|^2 \end{aligned} \quad (D3)$$

and after some basic algebra, this expression dramatically simplifies yielding Eq. (54).

Appendix E: Computation of the time-integrated probability of coincident counts for non-monochromatic light quanta

We replace into Eq. (54) the Gaussian waveforms given by Eqs. (29) and (30) and set $\tau_e = 0$ *i.e.* we have simultaneously impinging light quanta on beam splitter BS₁. Expanding now the mod-square yields

$$\begin{aligned} P_c(t_0, \tau_1, \tau_2) = & \frac{1}{16} \frac{2}{\pi \sigma^2} \left(e^{-4\frac{t_0^2}{\sigma^2}} - e^{-2\frac{t_0^2}{\sigma^2}} e^{-2\frac{(t_0 - \tau_1)^2}{\sigma^2}} e^{-2i\omega\tau_1} - e^{-2\frac{t_0^2}{\sigma^2}} e^{-2\frac{(t_0 - \tau_2)^2}{\sigma^2}} e^{-2i\omega\tau_2} \right. \\ & + e^{-2\frac{t_0^2}{\sigma^2}} e^{-2\frac{(t_0 - \tau_1 - \tau_2)^2}{\sigma^2}} e^{-2i\omega(\tau_1 + \tau_2)} - e^{-2\frac{t_0^2}{\sigma^2}} e^{-2\frac{(t_0 - \tau_1)^2}{\sigma^2}} e^{2i\omega\tau_1} + e^{-4\frac{(t_0 - \tau_1)^2}{\sigma^2}} + e^{-2\frac{(t_0 - \tau_2)^2}{\sigma^2}} e^{-2\frac{(t_0 - \tau_1)^2}{\sigma^2}} e^{2i\omega(\tau_1 - \tau_2)} \\ & - e^{-2\frac{(t_0 - \tau_1)^2}{\sigma^2}} e^{-2\frac{(t_0 - \tau_1 - \tau_2)^2}{\sigma^2}} e^{-2i\omega\tau_2} - e^{-2\frac{t_0^2}{\sigma^2}} e^{-2\frac{(t_0 - \tau_2)^2}{\sigma^2}} e^{2i\omega\tau_2} + e^{-2\frac{(t_0 - \tau_2)^2}{\sigma^2}} e^{-2\frac{(t_0 - \tau_1)^2}{\sigma^2}} e^{2i\omega(\tau_2 - \tau_1)} + e^{-4\frac{(t_0 - \tau_2)^2}{\sigma^2}} \\ & - e^{-2\frac{(t_0 - \tau_2)^2}{\sigma^2}} e^{-2\frac{(t_0 - \tau_1 - \tau_2)^2}{\sigma^2}} e^{-2i\omega\tau_1} + e^{-2\frac{t_0^2}{\sigma^2}} e^{-2\frac{(t_0 - \tau_1 - \tau_2)^2}{\sigma^2}} e^{2i\omega(\tau_1 + \tau_2)} - e^{-2\frac{(t_0 - \tau_1)^2}{\sigma^2}} e^{-2(t_0 - \tau_1 - \tau_2)^2} e^{2i\omega\tau_2} \\ & \left. - e^{-2\frac{(t_0 - \tau_2)^2}{\sigma^2}} e^{-2(t_0 - \tau_1 - \tau_2)^2} e^{2i\omega\tau_1} + e^{-4\frac{(t_0 - \tau_1 - \tau_2)^2}{\sigma^2}} \right) \end{aligned} \quad (E1)$$

In order to perform the time integration of this expression we will be using the formula

$$\int_{-\infty}^{\infty} e^{-2\frac{(y-a)^2}{\sigma^2}} e^{-2\frac{(y-b)^2}{\sigma^2}} dy = \frac{\sigma\sqrt{\pi}}{2} e^{-\frac{(a-b)^2}{\sigma^2}} \quad (E2)$$

valid for any $a, b \in \mathbb{R}$ and $\sigma \in \mathbb{R}^*$. Time-integrating Eq. (E1) and using cosines instead of complex exponentials takes us to

$$P_c(\tau_1, \tau_2) = \frac{1}{8\sigma\sqrt{\pi}} \left(2 - 2e^{-\frac{\tau_1^2}{\sigma^2}} \cos(2\omega\tau_1) - 2e^{-\frac{\tau_2^2}{\sigma^2}} \cos(2\omega\tau_2) \right. \\ \left. + e^{-\frac{(\tau_1+\tau_2)^2}{\sigma^2}} \cos(2\omega(\tau_1 + \tau_2)) + e^{-\frac{(\tau_1-\tau_2)^2}{\sigma^2}} \cos(2\omega(\tau_1 - \tau_2)) \right) \quad (\text{E3})$$

In order to obtain the τ_d -integrated expression we should have tackled Eq. (D2), an expression far too complicated for manual computation. Nonetheless, we can reasonably assume that each term from Eq. (E3) has a $e^{-\tau_d^2/\sigma^2}$ factor that was ignored (since we considered only the case $\tau_d = 0$), therefore, if we were to perform the time-integration over τ_d in the general case, we should get an extra factor of $\sigma\sqrt{\pi}$, yielding the probability of coincident counts

$$P_c(\tau_1, \tau_2) = \frac{1}{8} \left(2 - 2e^{-\frac{\tau_1^2}{\sigma^2}} \cos(2\omega\tau_1) - 2e^{-\frac{\tau_2^2}{\sigma^2}} \cos(2\omega\tau_2) \right. \\ \left. + e^{-\frac{(\tau_1+\tau_2)^2}{\sigma^2}} \cos(2\omega(\tau_1 + \tau_2)) + e^{-\frac{(\tau_1-\tau_2)^2}{\sigma^2}} \cos(2\omega(\tau_1 - \tau_2)) \right) \quad (\text{E4})$$

At this final stage, this expression was obtained by guess and plausibility arguments, nonetheless the full expression of Eq. (D2) was implemented on a computing machine, numerically time-integrated (over t_0 and τ_d) then compared to Eq. (E4). No differences were found.

-
- [1] R. Loudon, *The Quantum Theory of Light*, (Oxford University Press, Third Edition, 2003).
 - [2] L. Mandel, E. Wolf, *Optical Coherence and Quantum Optics*, (Cambridge, 1995).
 - [3] G. Grynberg, A. Aspect, C. Fabre, *Introduction to Quantum Optics: From the Semi-classical Approach to Quantized Light*, (Cambridge University Press, 2010).
 - [4] C. Gerry, P. Knight, *Introductory Quantum Optics*, (Cambridge, 2004).
 - [5] P. Grangier, G. Roger, A. Aspect, *Europhys. Lett.*, **1**, 173 (1986).
 - [6] A. Aspect, P. Grangier, *One-Photon Light Pulses versus Attenuated Classical Light Pulses* in “International Trends in Optics”, pp. 247-265, J. W. Goodman ed., (Academic Press, 1991).
 - [7] H. Kimble, M. Dagenais, L. Mandel, *Phys. Rev. Lett.* **39**, 691-695 (1977).
 - [8] R. Ghosh, L. Mandel, *Phys. Rev. Lett.* **59**, 1903 (1987).
 - [9] C. Hong, Z. Ou, L. Mandel, *Phys. Rev. Lett.* **59**, 18 (1987).
 - [10] R. Glauber, *Phys. Rev.* **130**, 6 (1963).
 - [11] E. Sudarshan, *Phys. Rev. Lett.* **10**, 277-279 (1963).
 - [12] R. Glauber, *Phys. Rev.* **131**, 6 (1963).
 - [13] H. Yuen, J. Shapiro, in *Coherence and Quantum Optics IV*, L. Mandel and E. Wolf, eds. (Plenum, 1978), p. 719.
 - [14] H. Yuen, V. Chan, *Opt. Lett.*, **8**, 3 (1983).
 - [15] U. Leonhardt, H. Paul, *Prog. Quant. Electr.* **19**, 89-130 (1995).
 - [16] C. Cohen-Tannoudji, J. Dupont-Roc, G. Grynberg, *Photons and Atoms: Introduction to Quantum Electrodynamics*, (Wiley-Interscience, New York, 1997).
 - [17] B. Yurke, S. McCall, J. Klauder, *Phys. Rev. A*, **33**, 4033 (1986).
 - [18] R. Campos, B. Saleh, M. Teich, *Phys. Rev. A*, **40**, 3 (1989).
 - [19] J. Rarity *et al.*, *Phys. Rev. Lett.* **65**, 11 (1990).
 - [20] J. Franson, *Phys. Rev. A*, **44**, 4552 (1991).
 - [21] M. Scully, K. Drühl, *Phys. Rev. A* **25**, 4 (1982).
 - [22] Y.-H. Kim, R. Yu, S. Kulik, Y. Shih, M. Scully, *Phys. Rev. Lett.* **84**, 1 (2000).
 - [23] S. Walborn *et al.*, *Phys. Rev. A* **65**, 033818 (2002). [arXiv:quant-ph/0106078](#)
 - [24] V. Jacques *et al.*, *New J. Phys.* **10**, 123009 (2008).
 - [25] A. Elitzur, L. Vaidman, *Found. Phys.* **23**, 9 (1993).
 - [26] P. Kwiat *et al.*, *Phys. Rev. Lett.* **74**, 4763-4766 (1995).
 - [27] S. Gleyzes *et al.*, *Nature* **446**, 297-300 (2007). [arXiv:quant-ph/0612031](#)
 - [28] A. Steinberg, P. Kwiat, R. Chiao, *Quantum Optical Tests of the Foundations of Physics in Atomic, Molecular, and Optical Physics*, pp 901-918 (Drake ed.), (AIP Press, 1996).
 - [29] P. Kwiat, A. Steinberg, R. Chiao, *Phys. Rev. A* **45**, 7729 (1992).
 - [30] L. Mandel, E. Sudarshan, E. Wolf, *Proc. Phys. Soc.* **84**, 435 (1964).
 - [31] R. Hanbury-Brown, R. Twiss, *Proc. Roy. Soc. (London)* **A242**, 300 (1957).
 - [32] H. Fearn, R. Loudon, *J. Opt. Soc. Am. B*, **6**, 5 (1989)
 - [33] J. Rarity, P. Tapster, R. Loudon, *J. Opt. B: Quantum Semiclass. Opt.* **7** S171 (2005) [arXiv:quant-ph/9702032](#)
 - [34] T. Pittman *et al.*, *Phys. Rev. Lett.* **77**, 10 (1996).
 - [35] Y.-H. Kim *et al.*, *Phys. Rev. A* **60**, R37-R40 (1999). [arXiv:quant-ph/9903048](#)
 - [36] Y.-H. Kim, *Phys. Lett. A*, **315**, 352-357 (2003). [arXiv:quant-ph/0304030](#)
 - [37] J. Bylander, I. Robert-Philip, I. Abram, *Eur. Phys. J. D*, **22**, 295-301 (2003).
 - [38] R. Feynman, R. Leighton, M. Sands, *The Feynman Lectures on Physics, Vol. III*, (Addison Wesley, 1965).
 - [39] M. Raymer *et al.*, *Opt. Commun.* **283**, 747-752 (2010).

- [arXiv:1002.0350 \[quant-ph\]](#)
- [40] K. Blow, R. Loudon, S. Phoenix, T. Shepherd, Phys. Rev. A **42**, 4102-14 (1990).
- [41] R. Campos, B. Saleh, M. Teich, Phys. Rev. A, **42**, 7 (1990).
- [42] T. Legero, T. Wilk, A. Kuhn, G. Rempe, Appl. Phys. B **77**, 797-802 (2003). [arXiv:quant-ph/0308024](#)
- [43] T. Legero, T. Wilk, A. Kuhn, G. Rempe, *Characterization of Single Photons Using Two-Photon Interference* in *Advances in Atomic, Molecular, and Optical Physics*, G. Rempe and M. Scully (eds.), (Academic Press, 2006). [arXiv:quant-ph/0512006](#)